Preparation of a-GeO_x:H alloys: Vibrational, optical, and structural properties

M. Zacharias and J. Bläsing
Institut für Experimentelle Physik, Fachbereich Festkörperphysik, Otto-von-Guericke Universität Magdeburg, Postfach 4120, 39016 Magdeburg, Germany
(Received 2 June 1995)

The preparation and systematic investigation of amorphous GeO_x:H alloys are described. Radial distribution fuctions show the broadening of the distances of the nearest neighbors and the restructuring of the third- and fourth-neighbor sites with increasing oxygen content. The static refractive index (3.7–2.4) and the Tauc gap (1.03–1.37) varied significantly with the preparation conditions, e.g., the oxygen content. The variation of the static refractive index from 2.05 to 2.6 with rising substrate temperature from 100 to 225 °C reflects density alterations of around 8%. The assignment of the infrared modes related to germanium, oxygen, and hydrogen is summarized. The IR spectra display modes that can be characterized as mainly oxygen modes. Ge-H bond configurations are not detectable. The peak position of the Ge-O-Ge stretching band shifts from 750 to 810 cm^{-1} with increasing oxygen content. The integrated absorption is analyzed in dependence on the oxygen content.

I. INTRODUCTION

Amorphous materials such as a-Si:H or a-Ge:H do not have the regular atomic structure typical for crystals. Recently, the x-ray diffraction patterns of various silicon-based thin films were measured.[1] The influence of hydrogen on the behavior of a-Si:H has been studied very intensively.[2–5] Most of the features of the amorphous network structure arise out of the details of the deposition process. Ternary a-Si(O,H) alloys have been prepared by the glow-discharge technique[6,7] or by sputtering[6,8] and the bonding of oxygen and hydrogen has been studied by IR spectroscopy. Ternary nonstochiometric alloys of a-Ge(O,H) have received much less attention up to now.[6] The differences in the bonding arrangement in a-Ge(O,H) alloys with respect to the corresponding a-Si(O,H) alloy films reflect differences in the plasma chemistry including temperature-dependent reactions at the growth surface. The most important differences derive from the role that disiloxane plays in Si,H,O chemistry and the absence of a similar role for digermoxane in Ge,H,O chemistry, as discussed for the glow-discharge process.[7] On the other hand, there has been interest in understanding the structure and vibrational modes (Raman, infrared) of glasses[9–11] both theoretically and experimentally.

Recently, strong visible photoluminescence has been reported for nanocrystalline Ge embedded in SiO_2 films[12,13] or nanocrystalline Ge formed by H_2 reduction of chemical-vapor-deposited $Si_{0.6}Ge_{0.4}O_2$ alloys.[14] The preparation of a-Si(Ge,O,H) alloys was a possible method to create Ge clusters in an amorphous Si(O,H) matrix. By following a thermal annealing of the Si(Ge,O,H) alloys the growth of Ge nanocrystals embedded in an amorphous SiO_x host matrix was induced.[15]

The presented systematic investigation of the a-GeO_x:H alloys is related to the above process. In contrast to Refs. 6 and 7 we have focused here on films with a high oxygen content, typically greater than 10 at. %, and a hydrogen content lower than 3 at. %.

II. FILM PREPARATION AND CHARACTERIZATION

The GeO_x:H alloys were prepared by dc magnetron sputtering using a crystalline germanium target and water as oxygen and hydrogen source. Thin amorphous films were grown on crystalline Si and on Corning glass with a film thickness of typically 1 μm. The influence of the preparation conditions on the properties of the resulting alloy films was investigated. The films were sputtered with a constant argon partial pressure of 0.8 Pa. Three deposition cycles were performed under the following variations.

Set 1: a water partial pressure from 20 to 340 mPa (with a constant substrate temperature T_S of 200 °C and a dc power of 60 W).

Set 2: a substrate temperature from 100 to 225 °C (with a water pressure of 350 mPa and a dc power of 60 W).

Set 3: a dc power from 40 to 120 W (with a water pressure of 200 mPa and a substrate temperature of 200 °C).

The amorphous character of the Ge alloy films was attested by x-ray diffraction under grazing incidence. An x-ray gonimeter URD 6 with Seeman-Bohlin geometry was used for the thin-film analysis of our Ge alloys. The angle of the grazing incidence was 1°. The Soller collimator for the analysis of the interference field worked with a divergence of 0.38°. The x-ray intensity was measured by means of a secondary monochromator and a scintillation counter tube. The cobalt $K\alpha$ radiation was used for the analysis.

The alloy concentration of films of set 1 was investigated using secondary neutral mass spectrometry (SNMS).[16,17] The quantitative analysis of the samples was realized using a calibration standard. Optical transmission measurements were performed using a Shimadzu

0163-1829/95/52(19)/14018(7)/$06.00 ©1995 The American Physical Society

spectrophotometer in the 0.3–2.5 μm wavelength region. We calculated the sample thickness, the dispersion of the refractive index, and the optical Tauc gap following the methods described earlier.[18–20,8] The refractive index $n(\lambda)$ was determined following the method of Manifacier, Gasiot, and Fillard.[18] Wemple and DiDomenico[19] developed the concept of the single-oscillator dispersion of the electronic dielectric constant. The refractive index at a photon energy $h\nu$ can be expressed in the form

$$n^2(h\nu)-1=\frac{E_d E_0}{E_0^2-(h\nu)^2} . \quad (1)$$

The energy parameters E_d and E_0 describe the dispersion of the refractive index and the single-oscillator energy, respectively. The refractive-index behavior in tetrahedrally bonded materials, as derived by the dispersion energy E_d, is not affected significantly by the loss of the long-range order.[20] The single-oscillator energy E_0 and static refractive index n_{stat} resulted as the long-wavelength limit by extrapolation of Eq. (1) to zero photon energy.

Infrared transmission was measured by means of a conventional IR double-beam spectrophotometer in the 300–4000 cm^{-1} region. The spectral resolution was approximately 2 cm^{-1} and the transmission data were accurate to 0.5%. As described in Ref. 21, the absorption-free transmission baseline was calculated and enables the determination of the absorption spectra with a minimization of errors due to features of interference.

The glow-discharge decomposition of the water molecules into the sputtering atmosphere leads to the incorporation of hydrogen and oxygen into the growing germanium alloys. As a result we noticed a variety of hydrogen and oxygen bonding to germanium. Table I summarizes the peak positions of the oxygen- and hydrogen-related infrared vibration modes reported previously. We have calculated the integrated absorption of the Ge-O-Ge stretching mode at around 750 cm^{-1}. A calibration constant which correlates the oxygen concentration and the integrated absorption has not been published in the past. Hence the change of integrated absorption and shift of the peak position were analyzed in dependence on the water partial pressure and the oxygen content.

III. EXPERIMENTAL RESULTS

The deposition rate of set 1 slightly decreased from 0.4 to 0.3 nm/s with increasing water pressure. The increase of the substrate temperature from 100 to 225 °C did not influence the deposition rate significantly.

The amorphous structure of the GeO$_x$:H was clearly proved by x-ray diffraction. Figure 1 shows the x-ray diffraction spectra of four Ge alloy films with increasing oxygen content. After correction due to air and substrate scattering and normalization to the actual GeO$_x$ gas curve, the curves were transformed into radial density distribution functions (RDF's) represented in reduced form without the average radial density $4\pi\rho r^2$. Two typical effects are connected with the increasing oxygen content, first [see Fig. 2(a)] the increase of the half-width of the first-neighbor peak and second [see Fig. 2(b)] the continuous rebuilding of the former neighbor sites.

Figure 3 shows the static refractive index n_{stat} of the films of set 1 as a function of the oxygen content. The static refractive index n_{stat} decreases nearly linearly from 3.7 to 2.4 by changing the water partial pressure from 20 to 340 mPa (Fig. 3). An increase of the Tauc gap E_T was observed from 1.03 to 1.37 eV for the same samples. As visible in Fig. 4, the decrease of the substrate temperature from 225 to 100 °C (set 2) is correlated with a decrease of the static refractive index n_{stat} from 2.6 to 2.05. The calculated Tauc gap E_T of set 2 shifted slightly from 1.24 and 1.39 eV. The variation of the dc power from 40 to 120 W (set 3) results in a weak increase of the static refractive index from 2.8 to 3.0. A Tauc gap of around 1.1 eV was calculated for samples of set 3 nearly independent on the dc power.

The IR transmission spectra of all films show peaks at around 510, 750, and 3400 cm^{-1}. The band of the hydroxyl group around 3400 cm^{-1} was not significant in intensity. A brand at around 1880 cm^{-1} which is known for Ge-H stretching vibrations was not detected. Figure 5 displays the dependence of the absorption coefficient in the wave number region from 400 to 1000 cm^{-1} for the samples of set 1. The peak position of the Ge-O-Ge asymmetric stretching mode shifted from around 750 to around 810 cm^{-1} with increasing oxygen content (Fig. 6).

TABLE I. Hydrogen- and oxygen-related infrared modes.

ω_{IR} (cm^{-1})	Assignment of the infrared mode
300	Ge-O-Ge rocking in a-Ge(O,H) alloys (Ref. 6)
500	Ge-O-Ge bending in a-Ge(O,H) alloys (Ref. 6)
560	Ge-H bond bending/rocking in a-Ge:H (Refs. 6,32)
670	coupled mode of a-Ge:H:O (Ref. 6)
750	Ge-O-Ge stretching in a-Ge(O,H) alloys (Ref. 6)
765/825	Ge-H doublet in a-Ge:H (Refs. 6,32)
860	Ge-O-Ge stretching in a-Ge(O,H) alloys prepared with water vapor (Ref. 6)
860	Ge-O-Ge asymmetric stretching in vitreous GeO$_2$ (Ref. 11)
1880	Ge-H stretching in a-Ge:H (Ref. 33)
2000	(GeH$_2$)$_n$ stretching in a-Ge:H (Refs. 6,32)
3400	O-H stretching (Ref. 34)

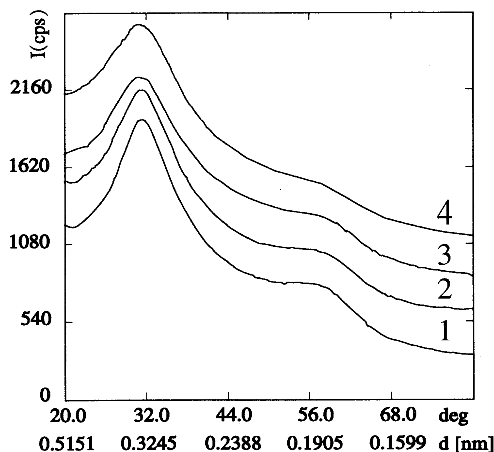

FIG. 1. X-ray diffraction spectra of GeO_x:H alloys with increasing oxygen content (1) 12, (2) 19.5, (3) 31, and (4) 45 at. %.

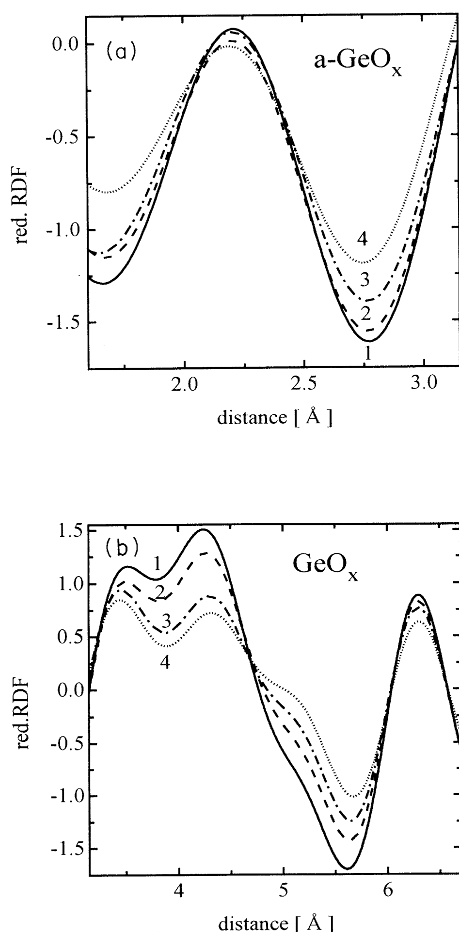

FIG. 2. Reduced RFD's of a-GeO_x alloy films with different oxygen content (1) 12, (2) 19.5, (3) 31, and (4) 45 at. %. (a) First part up to 3.15 Å; (b) second part from 3.15 to 6.7 Å.

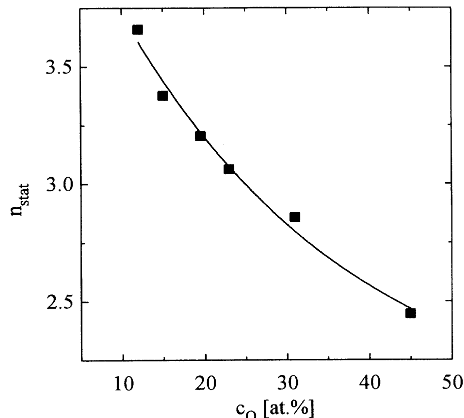

FIG. 3. Dependence of the static refractive index n_{stat} on the oxygen content (set 1) prepared with constant substrate temperature $T_S = 200\,°C$ and dc power $P_S = 60$ W.

Figure 7 shows the increase of the integrated absorption of the Ge-O-Ge stretching mode at around 760 cm^{-1}. The solid line in Fig. 7 is a fit guided by the eye. Within the sputtering plasma water is dissociated thermally into H atoms and OH radicals followed by a dissociation of the OH radicals. However, the broad band at around 3400 cm^{-1} indicates the presence of O-H bonding configurations in our thin-film materials.

The samples of set 1 were used for SNMS measurements. As a result we found an oxygen content from 12 to 45 at. % in correlation with the water partial pressure from 0.02 to 0.35 Pa. The error of the determination was ± 3 at. % and all the oxygen including that of the hydroxyl group was measured. However, the hydrogen content of the films was low. The integrated areas of the hydroxyl vibration mode around 3400 cm^{-1} of the samples were nearly identical. The fraction [O]/[Ge] of the samples increased from 0.14 to 0.82 and the difference in frequency between the peak positions of the Ge-O-Ge stretching mode was around 50 cm^{-1}.

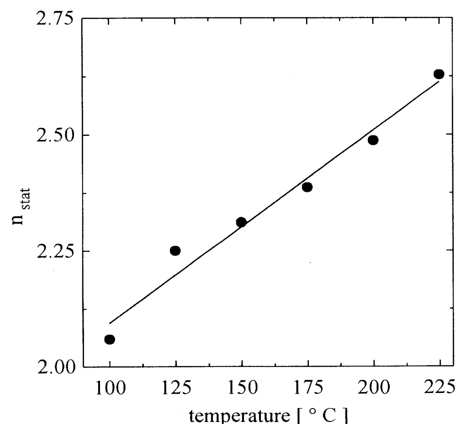

FIG. 4. The static refractive index n_{stat} as a function of the substrate temperature (set 2) prepared with a $p_{H_2O} = 350$ mPa and a dc power $P_S = 60$ W.

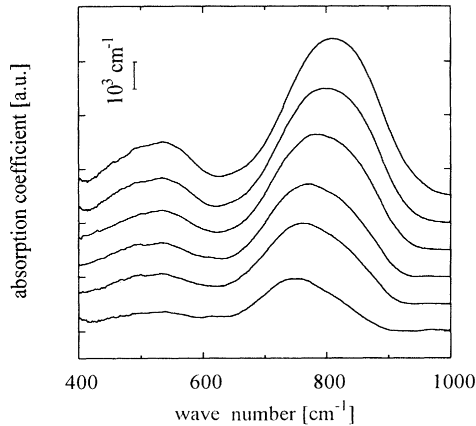

FIG. 5. Infrared absorption of the films of set 1.

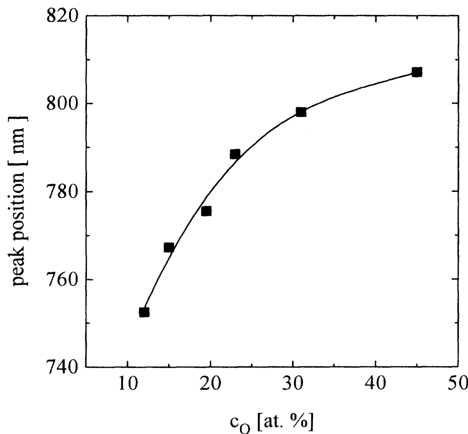

FIG. 6. Peak shift of the Ge-O-Ge stretching band with increasing oxygen content.

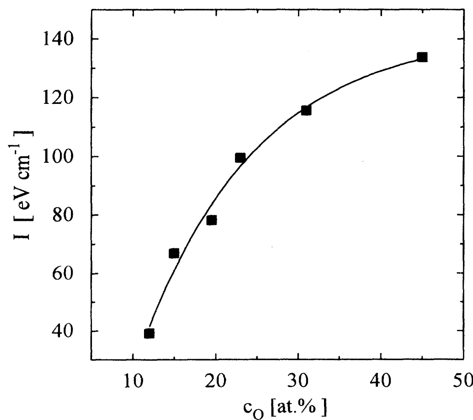

FIG. 7. Integrated absorption determined by the Ge-O-Ge stretching mode around 750 cm^{-1}.

IV. DISCUSSION

The x-ray pattern essentially describes the changes in the coordination of the atoms. A quantitative analysis is difficult because of the overlap of different partial scattering functions of the various elements. In crystalline Ge, the RDF up to $r=10$ Å exhibits well-defined, sharp peaks corresponding to shells of atoms separated by empty regions. This changes dramatically when going to amorphous Ge. Apart from the first peak due to the four nearest-neighbor atoms at $r=2.45$ Å, all crystalline correlation peaks broaden and merge into a smoother curve which follows the continuum parabola much more closely. On the other hand, it is known that the nearest-neighbor distance is well defined and close to the crystalline value, which was demonstrated by the qualitative agreement between the first RDF peak in crystalline versus amorphous germanium. The reason is that bond-length fluctuations in covalent amorphous semiconductors are very small (1–2 %).[22] In the case of our Ge/O alloys bond-length fluctuations greater than 1% or 2% should be included in further considerations. A simple estimation of a bond-angle variation as in pure amorphous Ge (Ref. 22) is not possible.

The detailed investigation of the reduced RDF's [Figs. 2(a) and 2(b)] makes it possible to quantify the structure deviations. The following distances were calculated as are result of the detailed modeling of the RDF: first neighbor (2.3 Å), second neighbor (3.3 Å), third neighbor (4.4 Å), fourth neighbor (5.3 Å), and fifth neighbor (6.4 Å). Figure 8(a) summarizes the relative broadening of all the nearest-neighbor zones with increasing oxygen content. The second visible effect [Fig. 8(b)] is the restructuring of the second- to fifth-neighbor sites. The modeling of the RDF's as a sum of Gaussian functions shows that only the third site is reduced in favor of the fourth site.

In Fig. 3 the dependence of the static refractive index n_{stat} on the oxygen content is shown. Indeed, it was found that the oxygen content of our films (up to 45 at. %) was far from the 67 at. % limit. Nevertheless, weak deviations from a linear relation of n_{stat} are indicated in Fig. 3. We note that there is evidence of a correlation between the oxygen content and the water partial pressure p_{H_2O} in the investigated parameter range. We have analyzed the dependence of the static refractive index n_{stat} in terms of the water partial pressure p_{H_2O}. The best fit seems to be a simple linear function for p_{H_2O} in the range of set 1:

$$n_{\text{stat}}=3.6-3.4\,\text{Pa}^{-1}p_{H_2O} \tag{2}$$

with a standard deviation of $\sigma=\pm 0.1$. The experimental error in determination of the static refractive index was around ± 0.1.

As shown in Fig. 4, the influence of substrate temperature from 100 to 225 °C causes an increase of n_{stat} from 2.05 to 2.6. But no clear correlation between the substrate temperature and the integrated absorption of the Ge-O-Ge stretching mode was detectable because of the scattering of the integrated absorption. Therefore the

measured tendency of n_{stat} with substrate temperature might not be directly related to the oxygen content. We investigated the density of the films of set 2 with x-ray total reflection. The densities of the films increased linearly with rising substrate temperature. Hence the n_{stat} versus T_S results reflect density alterations of around 8% with increasing substrate temperature.

The kinetics of the Ge, O, and H reactions were influenced not only by the physical sputtering processes but also by the etching of the growing films by the plasma. In the case of a high total pressure the growing and etching processes were nearly in balance, which causes a low growing rate and a columnar structure of the films. On the other hand, the mobility of the atoms on the growing surface was determined by the substrate temperature. Probably, at low temperatures low-density regions of the film are formed. Such processes could affect the microstructure and explain the increase of the static refractive index with the substrate temperature. A theoretical modeling of columnar growth has been performed recently.[23] Other forms of microstructure are known, such as the existence of voids, leading to a significant density deficit of amorphous semiconductors compared to the crystalline phase, or phase separation in compound materials. Although the microstructure influences many macroscopic qualities to a certain degree, such as density, diffusion, charge transport, optical properties, etc., it is difficult to describe this influence in a qualitative manner.[22]

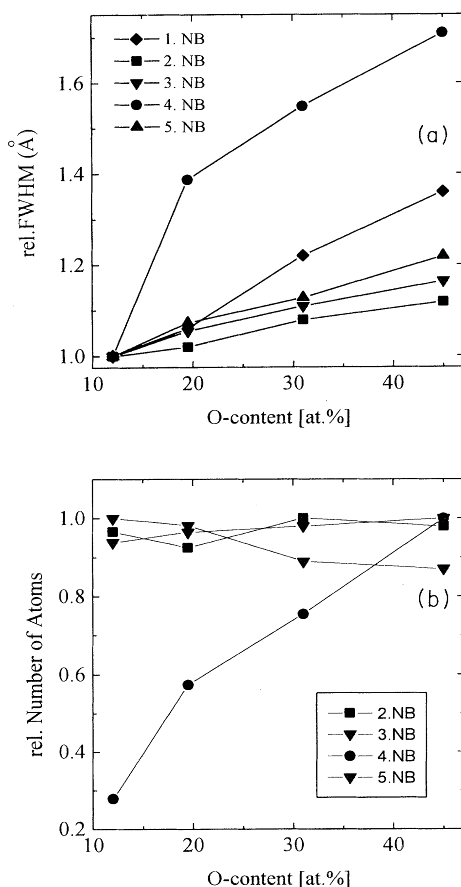

FIG. 8. Detailed investigation of the reduced RFD's of the samples. (a) Relative broadening of the peaks of the nearest neighbors with increasing oxygen content; (b) restructuring of the second- to fifth-neighbor sites.

The influence of the water pressure on the optical gap can be described by a linear equation in the range where the gap varies from 1.03 to 1.37 eV. The error of the gap determination was 0.05 eV. Indeed, we fitted for p_{H_2O} in the range from 0.02 to 0.35 Pa (set 1):

$$E_T(p_{H_2O})=E_T(0)+c_1 p_{H_2O} , \quad (3)$$

with $E_T(0)=1.0$ eV being the value of the Tauc gap extrapolated to zero oxygen (and hydrogen) content, respectively, and a slope of $c_1=0.93$ eV/Pa. The standard deviation of our approximation was $\sigma=\pm 0.05$.

Our value of $E_T(0)$ was higher than the 0.83 eV Tauc gap reported for sputtered unhydrogenated *a*-Ge.[24] A nearly linear dependence on H_2 partial pressure was found with a variation of the Tauc gap from 0.88 to around 1.1 eV.[25] However, our value of $E_T(0)$ agrees quite well with the above result considering the high oxygen content of our films used for the extrapolation. In analogy to the role of oxygen in amorphous SiO_x:H alloys,[26] it can be assumed that the increasing number of Ge-O bonds removes the weaker bonds from the top of the valence band and forms states deep in the valence band. The slight decrease of the optical gap with increasing substrate temperature might be considered as an effect of the microstructure.

The bond energy of Ge-H is given as 3.0 eV,[4,27] and the relevant value for O-H is 4.8 eV.[4] For the Ge-O bond energy a value of 4.7 eV was found.[28] The electronegativities for Ge, O, and H after Allred and Rochow[29] are 2.0, 3.5, and 2.2, respectively. That leads to the following differences of the electronegativities: Ge-O (1.5), Ge-H (0.2), and O-H (1.3). It is known that the greater the polarization of the binding the higher the binding energy. The enthalpy of formation of GeO_2 is 128.1 kcal/mol.[28] That value is low in comparison to the value of SiO_2 (203.4 kcal/mol) and GeO_2 is not stable in the same manner as SiO_2.

The band at 510 cm^{-1} has been assigned to the Ge-O-Ge bond bending vibration in *a*-Ge(O,H) alloys.[6] An overlap with the Ge-H bending vibration at 560 cm^{-1} can probably be excluded, and also the Ge-H stretching vibration of the monohydride group at 1880 cm^{-1} was not detectable. The broad band centered at 750 cm^{-1} has been assigned to the Ge-O-Ge asymmetric stretching band in *a*-Ge(O,H) alloys.[6] However, the known doublet (765/825 cm^{-1}) of the Ge-H bonding configuration of the dihydride group can probably be ruled out at this point and a lack of the 2000 cm^{-1} stretching band also ascribed to dihydride was found (Ref. 6 and references therein). A significant decrease of the dihydride group has already been reported for the preparation of *a*-Si:H films with water-saturated Ar in the trace impurities range below 1%.[30] A similar results was discussed previously[8] for the Si-H dihydride of SiO_x:H alloys, where the vibration of

the dihydride group was not found. In the presented case of a-GeO_x:H alloys, the relation of partial pressure between water and argon varied from 0.025 to 0.425 and resulted in a-$Ge_{1-x}O_x$:H films with around 45 at. % oxygen, finally. IR vibration bands ascribed to Ge-H groups were not found in our a-GeO_x:H films. The Ge-H stretching range around 1880 cm^{-1} (and 2000 cm^{-1}) indicated no significant amount of hydrogen directly bonded to Ge (lower than 2 at. %). We conclude that a high oxygen content restricts the bonding of hydrogen in agreement with Ref. 6. Thus the observed peak shift of the band around 510–520 cm^{-1} might be an effect of the bonding of more oxygen.

During the deposition the surface of the growing film was attacked by activated oxygen, i.e., oxygen admitted in the presence of a hot plasma which breaks the O_2 molecules. On the other hand, water was broken into hydrogen and hydroxyl. A small amount of this hydrogen bonded to an oxygen atom (Ge-O-H) as the films were grown. In the present case the main effect should be the influence of the higher electronegativity and bond energy of Ge-O and O-H related to Ge-H, so that the Ge-O bond configuration is preferred.

The oxygen was expected to occur as terminal as well as bridging oxygen. The charge transfer between 0 and Ge depends on the Ge-O-Ge bond angle. In vitreous GeO_2 the most probable value of the Ge-O-Ge angle was given at 128°.[11] The main bonding configuration observed in the investigated samples was the Ge-O-Ge vibration above 750 cm^{-1} as seen in Fig. 5. Contrary to Ref. 6 we did not find an oxygen-related infrared vibration at 860 cm^{-1}, which was reported as a special feature for a-Ge(H,O) films grown in a chamber with residual H_2O.

A peak shift of the Ge-O-Ge asymmetric stretching band is observable in Fig. 6 with increasing oxygen content (realized with variation of the water partial pressure). The results suggest a saturation of the mode as expected for the GeO_2 limit. However, some more information is needed about the development of the integrated absorption of the IR mode for oxygen content above 45 at. % to perform a realistic extrapolation of the saturation value. A similar effect of saturation was observed for the Si-O-Si asymmetric stretching mode of the a-SiO_x:H alloys.[31,8] In vitreous GeO_2 a peak position around 860 cm^{-1} was found corresponding to the infrared-active TO mode.[11,9] The deviation of our peak position may be an effect of the nonideal structure of the amorphous GeO_x network deposited with dc magnetron sputtering.

V. CONCLUSIONS

An increasing oxygen content is connected with a lowering of the state of order as provable by x-ray diffraction. The broadening of all the nearest-neighbor zones with increasing oxygen content is demonstrated. The modeling of the RDF shows a restructuring of the second- to fifth- neighbor sites. A strong correlation between the static refractive index n_{stat} and the deposition conditions was found. We note a nearly linear function between the static refractive index and the oxygen content of the films. An increasing substrate temperature causes an increase of the static refractive index correlated with the rising densities of the films. The IR spectra of the thin films show bands at 510, 750, and 3400 cm^{-1} assigned to the Ge-O bond bending, Ge-O-Ge bond stretching, and O-H stretching vibration, respectively. The Ge-H bonding configuration is not detectable. A significant peak shift of 60 cm^{-1} is found for the predominant Ge-O-Ge stretching vibration due to the increase of the oxygen content.

ACKNOWLEDGMENTS

The authors acknowledge W. Bock (Universität Kaiserslautern, FB Physik, Institut für Oberflächen- und Schichtanalytik) for performing the SNMS, A. Panckow and H. Freistedt (Universität Magdeburg, Institut für Experimantalphysik) for the helpful discusslon.

[1] E. Bustarret, M. Ligeon, and L. Ortéga, Solid State Commun. **83**, 461 (1992).
[2] E. C. Feeman and W. Paul, Phys. Rev. B **18**, 4288.
[3] M. Cardona, Phys. Status Solidi B **118**, 463 (1983).
[4] R. A. Street, *Hydrogenated Amorphous Silicon* (Cambridge University Press, Cambridge, England, 1991).
[5] T. D. Moustakas, in *Hydrogenated Amorphous Silicon. Part A: Preparation and Structure,* edited by J. Pankove, Semiconductors and Semimetals Vol. 21 (Academic, New York, 1984), p. 55.
[6] G. Lucovsky, S. S. Chao, J. Yang, J. E. Tyler, R. C. Ross, and W. Czubatyj, Phys. Rev. B **31**, 2190 (1985).
[7] G. Lucovsky, S. S. Chao, J. Yang, J. E. Tyler, and W. Czubatyj, J. Non-Cryst. Solids **66**, 99 (1984).
[8] M. Zacharias, T. P. Drüsedau, A. Panckow, H. Freistedt, and B. Garke, J. Non-Cryst. Solids **169**, 29 (1994).
[9] R. A. Barrio, F. L. Galeener, and E. Martinez, Phys. Rev. B **31**, 7779 (1985).
[10] M. F. Thorpe and F. L. Galeener, Phys. Rev. B **22**, 3078 (1980).
[11] F. L. Galeener, A. J. Leadbetter, and M. W. Stringfellow, Phys. Rev. B **27**, 1052 (1983).
[12] Y. Kanemitsu, J. Non-Cryst. Solids **164-166**, 639 (1993).
[13] Y. Kanemitsu, H. Uto, Y. Masumoto, and Y. Maeda, Appl. Phys. Lett. **61**, 2187 (1992).
[14] D. C. Paine, C. Caragianis, T. Y. Kim, and Y. Shigesato, Appl. Phys. Lett. **62**, 2842 (1993).
[15] M. Zacharias, J. Bläsing, J. Christen, and U. Wendt, J. Non-Cryst. Solids (to be published).
[16] H. Oechsner, in *Analysis of Microelectronic Materials and Devices,* edited by M. Grasserbauer and H. W. Werner (Wiley, New York, 1991), p. 493.
[17] M. Zacharias, F. Stolze, T. Drüsedau, and W. Bock, Phys. Status Solidi B **189**, 409 (1995).

[18]J. C. Manifacier, J. Gasiot, and J. P. Fillard, J. Phys. E **9**, 1002 (1976).
[19]S. H. Wemple and M. DiDomenico, Phys. Rev. B **3**, 1338 (1971).
[20]S. H. Wemple, Phys. Rev. B **7**, 3767 (1973).
[21]F. Stolze, M. Zacharias, S. Schippel, and B. Garke, Solid State Commun. **87**, 805 (1993).
[22]M. Stutzmann, in *Handbook on Semiconductors,* edited by S. Mahajan (Elsevier, Amsterdam, 1994).
[23]A. Mazor, D. J. Srolovitz, P. S. Hagan, and B. G. Bukiet, Phys. Rev. Lett. **60**, 424 (1988).
[24]L. J. Pilione, K. Vedam, J. E. Yehoda, and R. Messier, Phys. Rev. B **35**, 9368 (1987).
[25]T. P. Drüsedau and B. Schröder, J. Appl. Phys. **75**, 2864 (1994).
[26]W. Y. Ching, Phys. Rev. B **26**, 6610 (1982).
[27]G. Lucovsky, in *Fundamental Physics of Amorphous Semiconductors,* edited by F. Yonezawa, Springer Series in Solid State Science Vol. 25 (Springer New York, 1981), p. 87.
[28]*Germanium,* in Gmelin-Handbuch der Anorganischchen Chemie, Vol. 45 (Verlag-Chemie, Weinheim, 1958).
[29]J. D'Ans and E. Lax, in *Taschenbuch für Physiker und Chemiker,* edited by M. D. Lechner (Springer-Verlag, Berlin, 1992), Vol. 1, p. 473.
[30]C. Wang, G. N. Parsons, and G. Lucovsky, in *Amorphous Silicon Technology—1989,* edited by A. Madan, M. J. Thompson, P. C. Taylor, Y. Hamakawa, and P. G. LeComber, MRS Symposia Proceedings No. 149 (Materials Research Society, Pittsburgh, 1989), p. 75.
[31]D. V. Tsu, G. Lucovsky, and B. N. Davidson, Phys. Rev. B **40**, 1795 (1989).
[32]G. Lucovsky, R. J. Nemanich, and J. C. Knights, Phys. Rev. B **19**, 2064 (1979).
[33]G. Lucovsky, J. Yang, S. S. Chao, J. E. Tyler, and W. Czubatyj, Phys. Rev. B **28**, 3225 (1983).
[34]M. S. Brandt, H. D. Fuchs, M. Stutzmann, J. Weber, and M. Cardona, Solid State Commun. **81**, 307 (1992).